$\Delta(1232)$ electroproduction amplitudes in chiral soliton models of the nucleon

L. Amoreira*
Department of Physics, University of Beira Interior, P-6200 Covilhã, Portugal
and Center for Computational Physics, University of Coimbra, P-3000 Coimbra, Portugal

P. Alberto† and M. Fiolhais‡
Department of Physics and Center for Computational Physics, University of Coimbra, P-3000 Coimbra, Portugal
(Received 7 April 2000; published 5 September 2000)

The multipole amplitudes for the N-$\Delta(1232)$ electromagnetic transition are computed in the framework of the linear σ model and the chiral chromodielectric model for small and moderate photon virtualities. The models include quark and meson degrees of freedom and the nucleon and the Δ are clusters of three valence hedgehog quarks surrounded by meson clouds described by coherent states. Angular momentum and isospin projections are performed to endow model states representing the nucleon and the Δ with proper quantum numbers. Recoil corrections involved in the process $\gamma_v N \to \Delta$ are taken into account by performing linear momentum projection of the initial and final baryon states. The ratios $E2/M1$ and $C2/M1$ are in good agreement with the data in the two models, but the magnetic amplitude is better reproduced in the linear σ model. The ratios show little dependence with the model parameters. Both in the linear σ model and in the chromodielectric model the charged pions are responsible for the nonvanishing quadrupole-electric and -Coulomb amplitudes. The recoil corrections enhance the results obtained for the amplitudes without linear momentum projection, improving the comparison with experimental data. The dependence of the theoretical amplitudes with the choice of the reference frame is also studied.

PACS number(s): 13.40.Gp, 12.39.Fe, 14.20.Dh

I. INTRODUCTION

Electromagnetic processes have always played a central role in studies of the structure of nuclei, nucleons, and their excitations. Recently, the interest in the electroproduction of the $\Delta(1232)$ and other nucleon resonances has increased, fueled by the large number of experiments planned and already running in several centers (Mainz, Bonn, MIT, TJNAF, etc.), where very clean electromagnetic probes are now available. In this paper we report on a theoretical calculation of the multipole amplitudes of the N-Δ electromagnetic transitions.

The process $\gamma_v N \to \Delta$ has been considered in the framework of several models of baryon structure. From the point of view of a pure quark model, the Δ state results from a spin flip of one quark in the nucleon. This corresponds to a magnetic-dipole transition and vanishing quadrupole transitions. The experimental observation of quadrupole transitions, although small in comparison with the magnetic dipole, caused a discussion about the structure of the nucleon and the Δ. In models only with quarks, nonvanishing quadrupole electric and scalar nucleon-Δ transition amplitudes result from d-state admixtures to the quarks' lowest s state, otherwise those amplitudes would be identically zero [1–4]. The quadrupole transitions resulting from such charge deformations are generally small. However, other explanations can be found, in particular the contribution of pions included in the baryon model states [5–7], as in the type of effective theories considered in the present work.

Our calculations are carried on in the framework of two well known quark-meson models of the baryon structure, namely, the linear σ model (LSM) [8] and the chiral chromodielectric model (CDM) [9], which have been used to describe the structure of the nucleon [8–12]. In these models, a baryon — such as the nucleon — is a soliton with three bare valence quarks, all in the same orbital-spin-isospin state, interacting with chiral σ and $\vec{\pi}$ meson fields. In the CDM, there is an additional interaction with a scalar-isoscalar chiral singlet meson field — the chromodielectric field χ. Except for a small explicit chiral symmetry breaking term, both models are $SU(2)\times SU(2)$ chiral invariant, a symmetry which is spontaneously broken to $SU(2)$, the pions being the Goldstone bosons.

Although the two models use essentially the same ingredients, they provide quite different pictures of the nucleon (and of the delta). In the LSM the stability of the cluster of three quarks interacting with the mesons depends on the quark-meson interaction strength. A soliton is formed when the coupling constant for that interaction is sufficiently large, and it turns out that a strong meson cloud (particularly a pion cloud) is required for stabilizing the system. In the LSM, the chiral mesons bind the three quarks. In the CDM, in addition to the interaction between the quarks and the chiral mesons, there is an interaction between the chromodielectric field and the quarks. As a result of this interaction the quarks acquire a position-dependent dynamical mass which is an increasing function of the distance. The quarks are thus prevented to move too far away from the origin and such mechanism effectively generates quark confinement. The role of the chiral

*Electronic address: amoreira@mercury.ubi.pt
†Electronic address: pedro@teor.fis.uc.pt
‡Electronic address: tmanuel@teor.fis.uc.pt

mesons, although conceptually important to implement chiral symmetry and its dynamical breaking, gets much suppressed and the resulting picture of the baryon is a soliton with three confined valence quarks surrounded by a weak cloud of chiral mesons (particularly pions). By considering two models providing such extreme pictures of the nucleon, namely, with quite different meson clouds, we are able to address interesting questions, e.g., how electromagnetic transition amplitudes are sensitive to quantities such as the ''number of pions'' presented in the baryon states.

In the framework of the chiral models considered in this paper, the nucleon and the Δ are made out of neutral (σ, χ, and π^0) and charged (quarks and $\pi^{\pm}$) particles, the latter coupling directly to the electromagnetic probe (a virtual or a real photon). The three quarks are assumed in the same orbital-spin-isospin state occupying the lowest *s* state (no *d*-state admixture), represented by $|q\rangle$. Moreover the hedgehog state is assumed for the spin-isospin wave function of the quarks. The three valence quarks are therefore described by the fully symmetric state $|q^3\rangle$ (antisymmetrization applies in color space — the state is a Slater determinant in color space). A quantum mechanical description for the mesons is considered by means of coherent states representing pion, sigma and chi clouds, namely, $|\Pi\rangle$, $|\Sigma\rangle$, and $|\chi\rangle$. The starting point to describe a baryon in the framework of the LSM and CDM is, therefore, the Fock state $|\psi\rangle=|q\rangle^3|\Pi\rangle|\Sigma\rangle|\chi\rangle$. Such state should then be projected onto angular momentum and isospin eigenstates in order to get states with the nucleon and Δ quantum numbers [10–12].

The calculation reported in this work is a natural extension of Ref. [6]. We have refined the approximations, namely, by taking into account the state of motion of the initial and final baryon states involved in the nucleon-Δ transition. To this end, a linear momentum projection [13] of the initial and final baryon states is applied, following the method used in Ref. [14] for the calculation of the nucleon electromagnetic form factors. In addition to this conceptual improvement, we also present in more detail the formalism and address the issue of how the choice of the reference frame affects the theoretical transition amplitudes.

Other calculations of the electromagnetic N-Δ transition amplitudes carried out in several effective models of the nucleon have been reported in constituent quark models [1–4], with two-body exchange currents [15], in the Skyrme model [16,17], in the cloudy bag model [5,7], in chiral quark solitons of Nambu–Jona-Lasinio type with polarized Dirac sea [18,19], etc.

This paper is organized as follows. In Sec. II we give a short account of the models and sketch the approximations used to construct model states representing the nucleon and the delta. In Sec. III we develop the formalism for the application of the models to the electroproduction of the $\Delta(1232)$ with a special emphasis on the implementation of the linear momentum projection. Finally, the results are presented in Sec. IV together with their discussion. A summary of the main conclusions of this work is presented in Sec. V. The more technical aspects are given in the appendixes.

II. MODELS AND MODEL REPRESENTATION OF BARYONS

The Lagrangian densities of the LSM and the CDM can be written, in a compact form, as

$$\mathcal{L}=\mathcal{L}_q+\mathcal{L}_{\sigma,\pi}+\mathcal{L}_{q-\sigma,\pi,\chi}+\mathcal{L}_{\chi}, \tag{1}$$

where

$$\mathcal{L}_q=i\bar{\psi}\gamma^{\mu}\partial_{\mu}\psi, \tag{2}$$

$$\mathcal{L}_{\sigma,\pi}=\tfrac{1}{2}(\partial\sigma)^2+\tfrac{1}{2}(\partial\vec{\pi})^2-U(\sigma,\vec{\pi}) \tag{3}$$

are the pure quark and chiral meson terms,

$$\mathcal{L}_{q-\sigma,\pi,\chi}=\frac{g}{\chi^p}\bar{\psi}(\sigma+i\vec{\tau}\cdot\vec{\pi}\gamma_5)\psi \tag{4}$$

is the quark-meson interaction term, and

$$\mathcal{L}_{\chi}=\tfrac{1}{2}(\partial\chi)^2-\tfrac{1}{2}M_{\chi}^2\chi^2, \tag{5}$$

absent in the LSM, contains the kinetic and potential terms for the chromodielectric field. In these expressions $\psi(x)$ represents the quark field operator, $\vec{\pi}(x)$ and $\sigma(x)$ the chiral pion and sigma meson fields, respectively (the arrow denotes isovector), and $\chi(x)$ the chromodielectric field. The parameter p in the denominator of the interaction Lagrangian $\mathcal{L}_{q-\sigma,\pi,\chi}$ is 0 in the LSM (no χ field in this model) and 1 in the CDM.

The meaning of the other terms appearing in Eqs. (2)–(5) is the following. In Eq. (3), $U(\sigma,\pi)$ is the Mexican-hat potential, g in Eq. (4) is the coupling constant which is dimensionless in the LSM and has dimensions of energy in the CDM (with $p=1$). In Eq. (5) the second term on the right-hand side is just the mass term for the χ field, M_{χ} being its mass. Other versions of the CDM consider a potential which includes, in addition to the mass term, up to quartic terms in the χ field, as well as other powers of p in the interaction term (4). By just taking the mass term in the potential for χ and $p=1$ in the interaction, quark confinement is imposed in the smoothest way, which is the most appropriate choice for the quark matter sector of the CDM [20]. The Mexican-hat potential is given by

$$U=\frac{\lambda}{4}(\sigma^2+\vec{\pi}^2-\nu^2)^2+c\sigma+d. \tag{6}$$

The $SU(2)\times SU(2)$ chiral symmetry of $\mathcal{L}$ is explicitly broken by the small term $c\sigma$. The parameters λ, ν, and c are related to the sigma and pion masses m_{σ} and m_{π}, and to the pion decay constant f_{π}:

$$\lambda=\frac{m_{\sigma}^2-m_{\pi}^2}{2f_{\pi}^2},\quad \nu^2=f_{\pi}^2-\frac{m_{\pi}^2}{\lambda},\quad c=-f_{\pi}m_{\pi}^2. \tag{7}$$

In Eq. (6), d is a constant which guarantees that $\min U=0$. The Mexican hat potential induces spontaneous chiral sym-

metry breaking. The vacuum expectation values of the chiral fields are zero for the pion and $-f_\pi$ for the sigma:

$$\langle 0|\hat{\vec{\pi}}|0\rangle = 0, \tag{8}$$

$$\langle 0|\hat{\sigma}|0\rangle = -f_\pi \tag{9}$$

(we use the hat symbol whenever we want to stress the operatorial character of the fields). It is convenient to define a new sigma field, which we still denote by $\hat{\sigma}$, as the fluctuation around the vacuum value, i.e., we perform the replacement $\hat{\sigma} \to -f_\pi + \hat{\sigma}$. Hence, the vacuum expectation value of the ''new'' sigma field is zero, according to Eq. (9).

Altogether, the parameters of the models defined by Eq. (1) are the pion and σ masses (fixed at $m_\pi = 0.139$ GeV and $m_\sigma = 1.2$ GeV), the pion decay constant ($f_\pi = 0.093$ GeV), and g in the LSM and g and M_χ in the the CDM. In the simpler version of the CDM considered in this work, it turns out that the results are sensitive only to the combination $G = \sqrt{gM_\chi}$. The physical region of the coupling constant is $g \sim 5$ in the LSM [10,12] and $G \sim 0.2$ GeV, in the CDM [14,20]. We remark that the physical range of the coupling constant in the CDM is much narrower than in the LSM. For this reason, later on, in Sec. IV, when we show the dependence of the results on the coupling constant (all other parameters being fixed to the quoted values) we shall only consider the LSM. The only free parameters are g in the LSM and G in the CDM and these are fixed in order to reproduce well the bulk of the nucleon properties.

It is known that, in these quark-meson models, the Δ-nucleon mass splitting is small. We may remedy this by adding to the Hamiltonians of the models explicit bare baryon mass terms with different masses for the bare nucleon and the bare Δ [6,21]. Then there is one more parameter — the bare nucleon-bare Δ mass difference — which can be fitted to reproduce the physical nucleon Δ mass splitting. The inclusion of such a term has little effect (especially in the LSM) in the wave functions of both quarks and mesons. Such a bare nucleon-Δ mass splitting accounts for the residual chromomagnetic interaction and for the 't Hooft interaction which is attractive for the nucleon and absent in the Δ.

Solutions of the LSM and CDM representing the physical baryons can be obtained using a variational approach based on the projected hedgehog ansatz [11,12,21,22]. For the sake of completeness we sketch the formalism here. We consider three valence quarks with spin and isospin state in the so-called hedgehog configuration

$$|hh\rangle = \frac{1}{\sqrt{2}}(|u\downarrow\rangle - |d\uparrow\rangle). \tag{10}$$

All quarks occupy the same lowest positive energy s state of the model effective potential, given by the spinor

$$\langle \boldsymbol{r}|q_h\rangle = \frac{1}{\sqrt{4\pi}}\begin{pmatrix} u(r) \\ i\boldsymbol{\sigma}\cdot\hat{\boldsymbol{r}}v(r)\end{pmatrix}|hh\rangle. \tag{11}$$

In our approach, the pions, sigmas, and chis (in the CDM) are described by coherent states $|\Pi\rangle$ for the pions, $|\Sigma\rangle$ for the sigmas, and $|\chi\rangle$ for the chis. The expectation values of the field operators in these coherent states are the mean meson fields. The hedgehog ansatz for the mesons reads

$$\langle \Sigma|\hat{\sigma}(\boldsymbol{r})|\Sigma\rangle = \sigma(r), \tag{12}$$

$$\langle \Pi|\hat{\vec{\pi}}(\boldsymbol{r})|\Pi\rangle = \frac{\boldsymbol{r}}{r}\phi(r), \tag{13}$$

$$\langle \chi|\hat{\chi}(\boldsymbol{r})|\chi\rangle = \chi(r) \tag{14}$$

(we remember that $\hat{\sigma}$ is now the fluctuating part of the original sigma field around the vacuum expectation value $-f_\pi$). Actually the spherical symmetry of sigmas and chis and the ''hedgehoglike'' character of the pion with the peculiar isospin-coordinate space correlation, result from the quark spin-isospin hedgehog configuration (10) and from the requirement of minimum mean field energy solutions [21–23].

The pion coherent state is

$$|\Pi\rangle = N_\pi[\vec{\xi}]\exp\left\{\sum_{i=1}^{3}\int d^3\boldsymbol{k}\sqrt{\frac{\omega_\pi(k)}{2}}\xi_i(\boldsymbol{k})a_i^\dagger(\boldsymbol{k})\right\}|0\rangle, \tag{15}$$

where $a_i^\dagger(\boldsymbol{k})$ creates a free pion with momentum $\boldsymbol{k}$ and (Cartesian) isospin index i, N_π is a normalization factor, $\omega_\pi = \sqrt{k^2 + m_\pi^2}$, and $\xi_i(\boldsymbol{k})$ is the pion amplitude. Similarly, the sigma coherent state is given by

$$|\Sigma\rangle = N_\sigma[\eta]\exp\left\{\int d^3\boldsymbol{k}\sqrt{\frac{\omega_\sigma(k)}{2}}\eta(\boldsymbol{k})b^\dagger(\boldsymbol{k})\right\}|0\rangle, \tag{16}$$

where $b^\dagger(\boldsymbol{k})$ is the sigma creation operator, $\eta(\boldsymbol{k})$ is the coherent state amplitude function for the σ field. A similar expression holds for the chi field and we denote the amplitude of the corresponding coherent state by $\kappa(\boldsymbol{k})$.

The coherent states are particularly easy to deal with because they are eigenstates of the annihilation operators, e.g.,

$$a_i(\boldsymbol{k})|\Pi\rangle = \sqrt{\frac{\omega_\pi(k)}{2}}\xi_i(\boldsymbol{k})|\Pi\rangle. \tag{17}$$

Similar expressions hold, involving the annihilation operator of σ's and χ's.

The coherent state amplitudes are the Fourier transforms of the meson functions in coordinate space introduced in Eqs. (12)–(14), and exhibit the following hedgehog shape in momentum space:

$$\xi_i(\boldsymbol{k}) = -i\frac{k_i}{k}\xi(k), \tag{18}$$

$$\eta(\boldsymbol{k}) = \eta(k), \tag{19}$$

$$\kappa(\boldsymbol{k}) = \kappa(k). \tag{20}$$

Altogether the hedgehog baryon ansatz reads

$$|\psi_h\rangle = |q_h\rangle^3 |\Sigma\rangle |\Pi\rangle |\chi\rangle. \tag{21}$$

In the mean field approximation we demand the total energy functional $E = \langle \psi_h | :H: | \psi_h \rangle$, where $:H:$ is the normal ordered Hamiltonian of the models defined by Eq. (1), to be stationary with respect to variations of $u(r)$, $v(r)$, $\sigma(r)$, $\phi(r)$, and $\chi(r)$. Of course, the meson wave functions may equivalently be determined by performing the variations with respect to the coherent state amplitudes $\xi(k)$, $\eta(k)$, and $\kappa(k)$. The variations with respect to the functions of r lead to a set of differential equations. For appropriate choices of the coupling constants, soliton solutions of those equations are obtained with three quarks absolutely confined (in CDM) [9,11] or just bound (in LSM) [8,10].

The solitons described by the hedgehog state, $|\psi_h\rangle$ cannot represent physical baryons because they are not eigenstates of angular momentum or isospin. In addition, Eq. (21) represents a localized object and therefore the translational symmetry of the model Hamiltonians is also broken in such states. In particular they contain spurious center-of-mass components which contribute to the energy and to other observables.

States with good spin and isospin can be obtained from $|\psi_h\rangle$ by means of the Peierls-Yoccoz projection. The hedgehog only contains states with $J=T$ and therefore, due to such space-isospace correlation, a single projection, either in spin or in isospin, is needed [12,22]. We choose to project onto isospin. A baryon with isospin T, spin $J=T$ and projection quantum numbers t and s (for isospin and spin, respectively) is given by

$$|T,t;J=T,s\rangle = (-1)^{T+t} \mathcal{P}^T_{t-s} |\psi_h\rangle, \tag{22}$$

where $\mathcal{P}^T_{t-s}$ is the isospin operator

$$\mathcal{P}^T_{ts} = \frac{2T+1}{8\pi^2} \int d\Omega \mathcal{D}^{T*}_{ts}(\Omega) R(\Omega). \tag{23}$$

In this expression, $R(\Omega)$ stands for the rotation operator in isospin space, $\mathcal{D}$ are the Wigner matrices, and the integration is performed over all orientations Ω (which represents the set of three Euler angles in isospin space). In the following we consider $s=-t=M$ and use the shorthand notation $P_{JM} = \mathcal{P}^T_{M,M}$.

On the other hand, a model state representing a baryon at rest can be obtained by applying a Peierls-Yoccoz projection onto linear momentum zero to the state already projected onto isospin (and angular momentum). The Peierls-Yoccoz linear momentum projector is given by

$$P_{\boldsymbol{q}} = \frac{1}{(2\pi)^3} \int d\boldsymbol{a} e^{i\boldsymbol{a}\cdot\boldsymbol{q}} U(\boldsymbol{a}), \tag{24}$$

where $U(\boldsymbol{a})$ is the translation operator. A nucleon at rest is therefore represented by the model state

$$|J=T=\tfrac{1}{2},\ M,\boldsymbol{q}=0\rangle = P_{\boldsymbol{q}=0} P_{JM} |\psi_h\rangle = P_{\boldsymbol{q}=0} |\psi_{JM}\rangle. \tag{25}$$

For $\boldsymbol{q}=0$, the isospin-angular momentum projector operator and the linear momentum projector operator commute, but this is no longer the case for $\boldsymbol{q}\neq 0$ [24].

In order to include recoil effects in the calculations, in principle one should boost [13] the zero momentum states (25), but the technical difficulties associated with boosting prevent, in practice, the use of such a procedure. However, at least for small linear momentum $\boldsymbol{q}$, we may approximate the boost operation by the Peierls-Yoccoz projection onto linear momentum $\boldsymbol{q}$ [11,24]. Thus, the model state representing a physical baryon of angular momentum and isospin J and linear momentum $\boldsymbol{q}$ is

$$|J=T,M,\boldsymbol{q}\rangle \sim P_{\boldsymbol{q}} |\psi_{JM}\rangle. \tag{26}$$

Proper normalization of the projected state requires the inclusion of kinematical normalization factors. For example a nucleon with four-momentum q, $|N(q)\rangle$, is described by

$$|N(q)\rangle \to \sqrt{(2\pi)^3 \delta^3(0)} \sqrt{\frac{E}{m_N}} \frac{P_{\boldsymbol{q}} |\psi_{JM}\rangle}{\sqrt{\langle P_{\boldsymbol{q}} \psi_{JM} | P_{\boldsymbol{q}} \psi_{JM}\rangle}}, \tag{27}$$

where $J=\frac{1}{2}$, m_N is the nucleon mass and $E=\sqrt{q^2+m_N^2}$ its energy.

Before presenting the formalism to compute the amplitudes for the electroproduction of the delta, one should briefly mention how the radial profiles $u(r)$, $v(r)$, $\sigma(r)$, $\phi(r)$, and $\chi(r)$ are determined. They may be determined in the so-called ''variation-before-projection'' (VBP) method, and, in that case, the stationarity of the mean field energy is required. A better approach (even if much more demanding numerically) is the variation-after-projection (VAP) method, where the energy functional to be minimized is the expectation value of the normal ordered Hamiltonian in the projected state $|\psi_{JM}\rangle$. In this procedure, which we followed, one obtains different field radial profiles $u_B(r), v_B(r), \phi_B(r)$, $\sigma_B(r)$, $\chi_B(r)$ [and coherent state amplitudes $\xi_B(k), \eta_B(k)$, $\kappa_B(k)$] for the nucleon ($B \to N$) and for the delta ($B \to \Delta$). The results presented Sec. IV use the VAP method for the angular momentum projection and the approximate VAP method for the linear momentum projection as described in Ref. [11]. Unless otherwise stated, the coupling constants are $g=5$ in the LSM [8,12,25] and $G=0.2$ GeV in the CDM [14,20], for which nucleon properties are well described. These values, together with the abovementioned values for meson masses and pion decay constant, will be referred to as the *standard* parameters.

III. MULTIPOLE AMPLITUDES

The N-Δ electromagnetic transverse helicity amplitudes [26] are defined by

$$A_{\lambda}^{(\mu)} = -\frac{e}{\sqrt{2k_W}}\langle \Delta\tfrac{1}{2}\lambda;\boldsymbol{k}_\Delta|:\boldsymbol{\epsilon}_\mu\cdot\boldsymbol{J}(0):|N\tfrac{1}{2}\lambda-\mu;\boldsymbol{k}_N\rangle \tag{28}$$

and the scalar helicity amplitude by

$$S_\lambda = \frac{1}{\sqrt{2}}\frac{e}{\sqrt{2k_W}}\langle \Delta\tfrac{1}{2}\lambda;\boldsymbol{k}_\Delta|:J^0(0):|N\tfrac{1}{2}\lambda;\boldsymbol{k}_N\rangle, \tag{29}$$

where J^μ is the electromagnetic current density operator $\boldsymbol{\epsilon}_i$, $i=0,\pm1$ are the photon polarization vectors ($\boldsymbol{\epsilon}_0$ is chosen along the direction of the photon motion), and k_W is the magnitude of the photon three-momentum at the photon point [4]. Because of gauge invariance, the other amplitude — longitudinal amplitude — is just the scalar amplitude multiplied by the kinematical factor ω/k. The values for λ and μ are usually chosen as $\lambda=1/2,3/2$, $\mu=1$ for the transverse amplitudes and $\lambda=1/2$ for the scalar amplitude. If the linear momentum projection of the model states is skipped (i.e., no recoil corrections), expressions (28) and (29) reduce to those usually presented in the literature [see, e.g., Eq. (7) of Ref. [6]] using the procedure described in Ref. [25].

Replacing the baryon states above by their model representations in Eq. (27), and noting that $U^\dagger(\boldsymbol{r})J^\nu(0)U(\boldsymbol{r}) = J^\nu(\boldsymbol{r})$, we get (for $\lambda=1/2$, $\mu=1$)

$$A_{1/2} = -N_{N\Delta}\int d^3\boldsymbol{a}d^3\boldsymbol{r}e^{-i\boldsymbol{q}\cdot\boldsymbol{r}}\langle \Delta\tfrac{1}{2}\ \tfrac{1}{2}|U^\dagger[(x-1)\boldsymbol{a}]:\boldsymbol{\epsilon}_1\cdot\boldsymbol{J}(\boldsymbol{r}):U(x\boldsymbol{a})|N\tfrac{1}{2}\ -\tfrac{1}{2}\rangle, \tag{30}$$

$$S_{1/2} = \frac{1}{\sqrt{2}}N_{N\Delta}\int d^3\boldsymbol{a}d^3\boldsymbol{r}e^{-i\boldsymbol{q}\cdot\boldsymbol{r}}\langle \Delta\tfrac{1}{2}\ \tfrac{1}{2}|U^\dagger[(x-1)\boldsymbol{a}]:J^0(\boldsymbol{r}):U(x\boldsymbol{a})|N\tfrac{1}{2}\ \tfrac{1}{2}\rangle, \tag{31}$$

where x is the fraction of the photon momentum carried by the delta. In this way, the parameter x identifies the reference frame used in the calculations: $x=0$ corresponds to the delta rest frame which is mostly used in the literature. The factor $N_{N\Delta}$ contains all kinematical factors as well as the projected states normalization terms [see Eq. (27)], and is given by

$$N_{N\Delta} = \frac{1}{(2\pi)^3}\frac{e}{\sqrt{2k_W}}\sqrt{\frac{E_N}{m_N}}\sqrt{\frac{E_\Delta}{m_\Delta}}\frac{1}{\sqrt{F_{1/2}[(x-1)\boldsymbol{q}]F_{3/2}(x\boldsymbol{q})}}, \tag{32}$$

with

$$F_{1/2}(q) = \langle N\tfrac{1}{2}\ \tfrac{1}{2}|P_{\boldsymbol{q}}|N\tfrac{1}{2}\ \tfrac{1}{2}\rangle, \tag{33}$$

and similarly for the delta F factor. These factors only depend on the magnitude $|\boldsymbol{q}|$.

The multipole N-Δ transition amplitudes are usually extracted from the helicity amplitudes above making a multipole expansion of the electromagnetic field. For nucleon and delta model states which are eigenstates of the angular momentum and parity operators, only the magnetic dipole and the electric and scalar quadrupole terms contribute to the transition (see Appendix A for details). The linear momentum projection in our approach affects the rotational symmetry of the baryon states, and the relevant multipoles are not automatically selected. Instead, one has to explicitly remove the spurious terms in the multipole expansion of the exponential in Eqs. (30) and (31), which implies restricting the momentum transfer q to low values. In that case, the rotational symmetry of the model states is almost preserved even if the linear momentum projection is performed. The multipole amplitudes are then

$$M^{M1}(q) = -\tfrac{3}{2}N_{N\Delta}\int d^3\boldsymbol{a}d^3\boldsymbol{r}j_1(qr)\langle \Delta\tfrac{1}{2}\ \tfrac{1}{2}|U^\dagger[(x-1)\boldsymbol{a}]:[\hat{\boldsymbol{r}}\times\boldsymbol{J}(\boldsymbol{r})]_1:U(x\boldsymbol{a})|N\tfrac{1}{2}\ -\tfrac{1}{2}\rangle, \tag{34}$$

$$M^{E2}(q) = -\frac{\sqrt{10\pi}}{k}N_{N\Delta}\int d^3\boldsymbol{a}d^3\boldsymbol{r}\langle \Delta\tfrac{1}{2}\ \tfrac{1}{2}|U^\dagger[(x-1)\boldsymbol{a}]:[\boldsymbol{\nabla}\times j_2(qr)\boldsymbol{Y}^1_{22}(\hat{\boldsymbol{r}})]\cdot\boldsymbol{J}(\boldsymbol{r}):U(x\boldsymbol{a})|N\tfrac{1}{2}\ -\tfrac{1}{2}\rangle, \tag{35}$$

$$M^{C2}(q) = -\sqrt{10\pi}N_{N\Delta}\int d^3\boldsymbol{a}d^3\boldsymbol{r}j_2(qr)Y_{20}(\hat{\boldsymbol{r}})\langle \Delta\tfrac{1}{2}\ \tfrac{1}{2}|U^\dagger[(x-1)\boldsymbol{a}]:J^0(\boldsymbol{r}):U(x\boldsymbol{a})|N\tfrac{1}{2}\ \tfrac{1}{2}\rangle, \tag{36}$$

where $\boldsymbol{Y}^m_{jl}$ are the vector spherical harmonics, $j_l(x)$ are the spherical Bessel functions and the index 1 in the $M1$ operator denotes component $+1$ in the spherical basis. It is worth noticing that formulas (34)–(36) differ from those used when no recoil corrections are considered [see, e.g., Eqs. (10)–(12) of Ref. [6]] by the integration over $\boldsymbol{a}$ and by the presence of

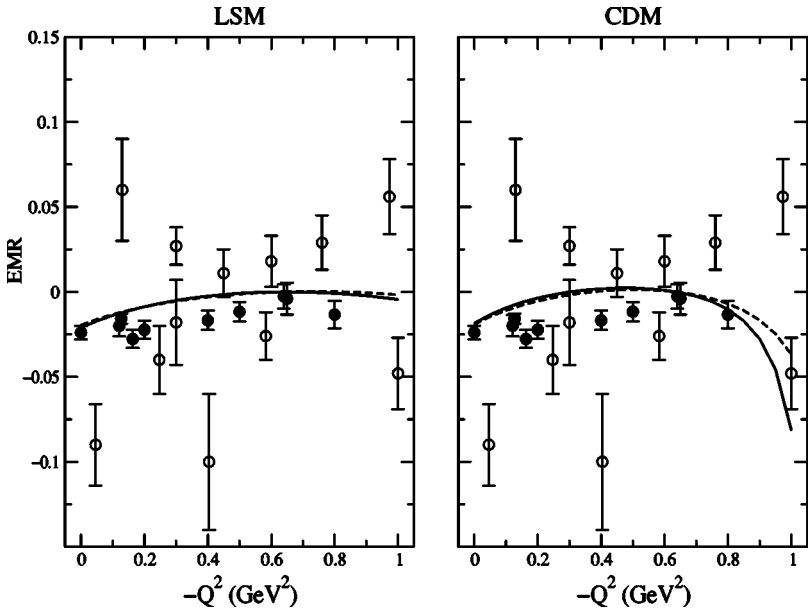

FIG. 1. Quadrupole electric to dipole magnetic ratio in the LSM and the CDM, as a function of $-Q^2$. The solid (dashed) lines show the results with (without) recoil effects for the standard parameter set and in the rest frame of the Δ. Experimental data was taken from Refs. [27,28] (○) and Refs. [29–31] (●).

the translation operations. Had we inserted $\delta^3(\boldsymbol{a})$ in Eqs. (34)–(36) and integrated over $\boldsymbol{a}$, the expressions for the multipole amplitudes when no recoil effects are considered (see, amongst others, Refs. [6,16,18,19]) would be obtained.

The electric quadrupole amplitude involves the operator

$$\hat{O}_{\mathrm{E2}}(q)=\frac{1}{q}\int d^3\boldsymbol{r}[\boldsymbol{\nabla}\times j_2(qr)\boldsymbol{Y}^1_{22}(\hat{\boldsymbol{r}})]\cdot\boldsymbol{J}(\boldsymbol{r}), \qquad (37)$$

which, using the properties of the vector spherical harmonics and integration by parts, can be written as

$$\hat{O}_{\mathrm{E2}}(q)=\frac{1}{\sqrt{6}}\frac{\omega}{q}\int d^3\boldsymbol{r}\frac{d}{dr}[rj_2(qr)]Y_{21}(\hat{\boldsymbol{r}})J^0(\boldsymbol{r})$$

$$-\frac{iq}{\sqrt{6}}\int d^3\boldsymbol{r}j_2(qr)Y_{21}(\hat{\boldsymbol{r}})\boldsymbol{r}\cdot\boldsymbol{J}(\boldsymbol{r}), \qquad (38)$$

where we used the electric current conservation condition to simplify the first term. The second term gives a negligible correction to the $E2$ amplitude in the low momentum regime and can be dropped [6]. Other technical aspects of the calculation of the multipole amplitudes are provided in Appendixes B and C.

IV. RESULTS AND DISCUSSION

The ratios $E2/M1$ and $C2/M1$ for the delta electroproduction are related to the multipoles (34)–(36) through

$$\frac{E2}{M1}=\frac{1}{3}\frac{M^{E2}}{M^{M1}} \qquad (39)$$

$$\frac{C2}{M1}=\frac{1}{2\sqrt{2}}\frac{M^{C2}}{M^{M1}}. \qquad (40)$$

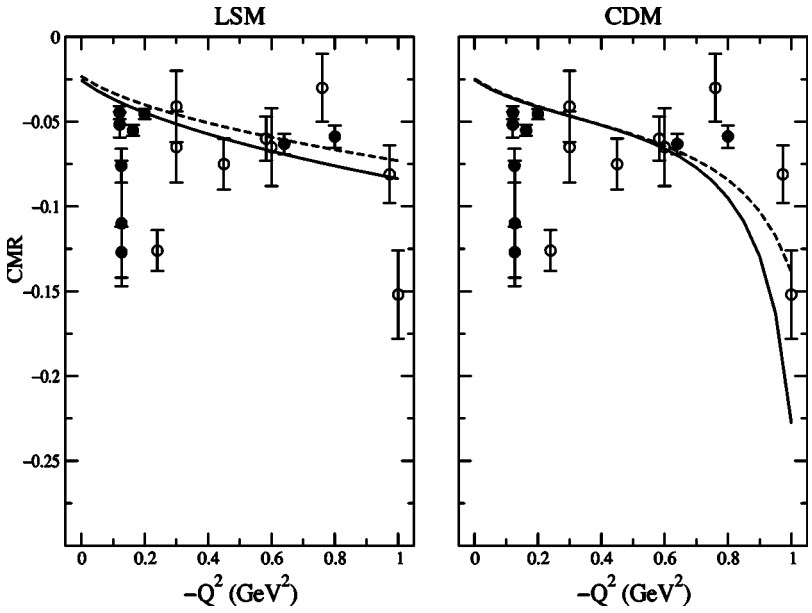

FIG. 2. Quadrupole Coulomb to dipole magnetic ratio. Conventions, parameters and reference frame as in Fig. 1. Experimental data taken from Refs. [27,32] (○) and Refs. [30,33] (●).

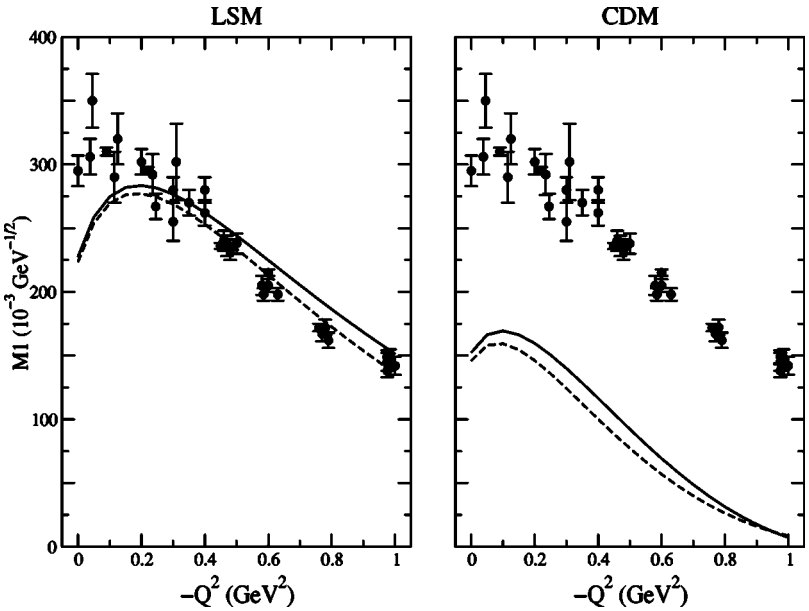

FIG. 3. Dipole magnetic amplitude $M1$ (in units of 10^{-3} GeV$^{-1/2}$) as a function of $-Q^2$, for the LSM and the CDM. Conventions, parameters, and reference frame as in Fig. 1. Experimental data taken from Ref. [34].

These ratios (EMR and CMR, respectively) are equal for $|\boldsymbol{q}|\to 0$, a limit which is never met since, even at the photon point, a finite $|\boldsymbol{q}|$ is needed for the transition to take place.

In most calculations reported in the literature the transition amplitudes are computed in the rest frame of the Δ. Such a choice corresponds to $x=0$ in the expressions of Sec. III. The nucleon four-momentum $(E_N,-\boldsymbol{q})$ and the photon four-momentum $(\omega,\boldsymbol{q})$ completely specify the kinematics and the (invariant) photon virtuality, $Q^2=-q^2$ is the appropriate quantity in terms of which the electroproduction amplitudes should be expressed. In the Δ reference frame,

$$|\boldsymbol{q}|^2=\left(\frac{m_\Delta^2+m_N^2+Q^2}{2m_\Delta}\right)^2-m_N^2 \tag{41}$$

and

$$\omega=\frac{m_\Delta^2-m_N^2-Q^2}{2m_\Delta}. \tag{42}$$

Figure 1 shows the results for the quadrupole electric to dipole magnetic ratio, in the LSM and CDM, for standard parameter sets in both models, in the rest frame of the delta. Figure 2 displays the quadrupole Coulomb to dipole magnetic ratio as a function of $-Q^2$. The first conclusion to be drawn is the compatibility of the model predictions with the data, namely, the negative signs for both ratios. From the theoretical point of view we do not find any sign of the up and down behavior of the data points. Another interesting conclusion is the small effect of the recoil corrections in EMR and CMR. Recoil corrections enhance the nucleon magnetic moments [11,24] and nucleon magnetic form factors [14]. Such enhancement is also found in the nucleon-Δ magnetic transition as it is shown in Fig. 3, improving the

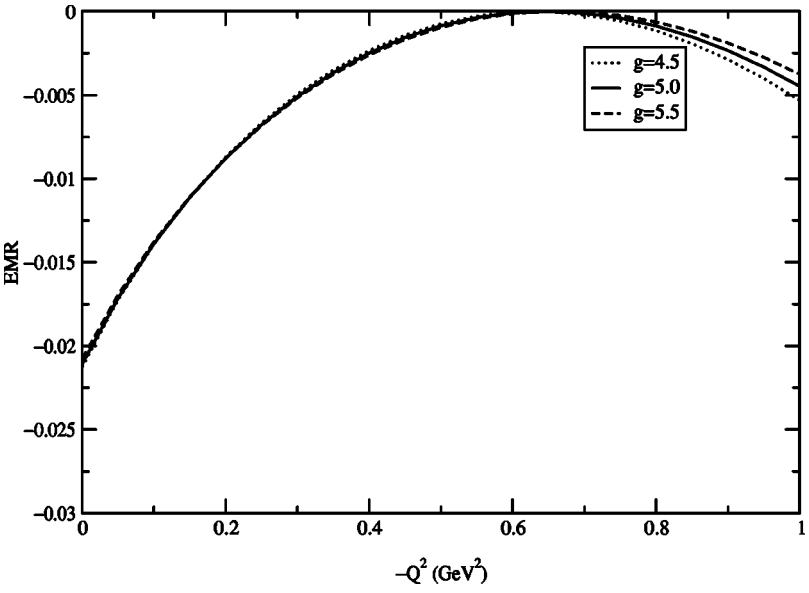

FIG. 4. EMR in the LSM for three values of the coupling constant.

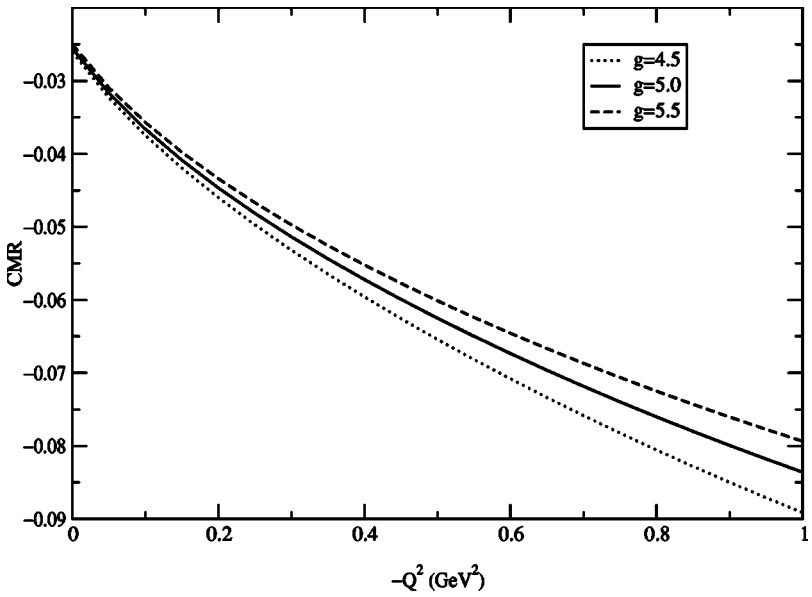

FIG. 5. CMR in the LSM for three values of the coupling constant.

comparison with experimental values, but the effect, in the present case, is smaller than for the nucleon.

A similar enhancement turns out to show up in the quadrupole electric and Coulomb multipoles, and altogether no sensible modification appears in EMR and CMR. In the CDM the modification of M^{M1} due to a better treatment of the kinematics of the nucleon and the Δ is not enough to achieve a better comparison with the data. The comparison with the data of this observable favors the model with large number of pions in the cloud. The big slope of the theoretical CMR in the CDM is due to the small value predicted for M^{M1} in this model.

The values of the ratios at the photon point (Δ photoproduction) are -2.56% (LSM) and -2.54% (CDM) for the CMR and -2.11% (LSM), -1.85% (CDM) for the EMR. These values are compatible (although slightly smaller, in the case of the EMR) with the experimental value $-2.5 \pm 0.5\%$ estimated for EMR by the Particle Data Group [35].

It is not our purpose to find fittings of model parameters that better reproduce the experimental results (model parameters were fixed in the nucleon sector of the models). Nevertheless it is interesting to analyze the dependence of the results with model parameters, namely, the coupling constants. As stated before, the physical window for G in the CDM is relatively narrow and the resulting radial wave functions are very much similar throughout that physical range. The LSM, on the other hand, provides a larger range and a large variety of radial wave functions. The results are summarized in Figs. 4–6 for three values of the coupling constant in the LSM: $g=4.5$ (weak coupling, weak pion cloud), $g=5.0$ (intermediate coupling, standard parameter), and $g=5.5$ (strong coupling, strong pion cloud). The graphs correspond to the calculation with recoil corrections. As Fig. 4 reveals, the EMR remains impressively unchanged with $-Q^2$. The CMR (Fig. 5) is affected specially for large $-Q^2$. The effect on $M1$ is shown in Fig. 6. The multipole

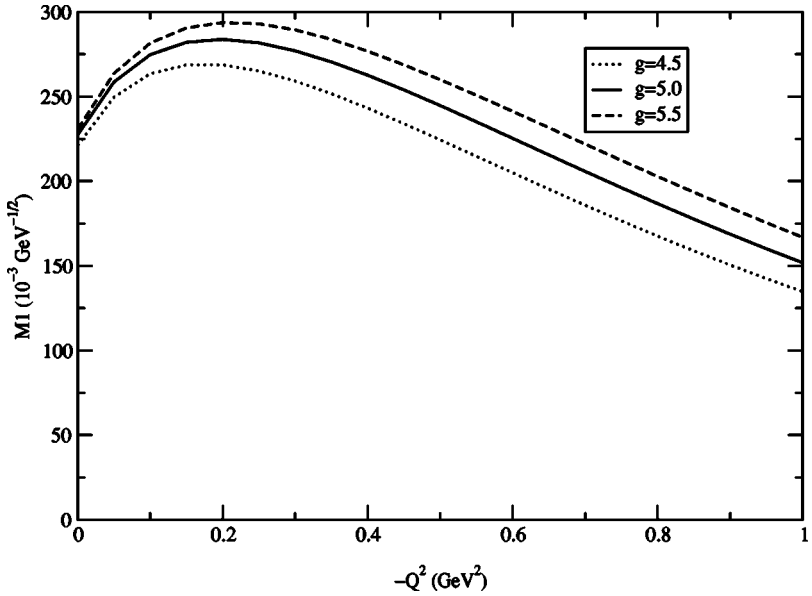

FIG. 6. $M1$ in the LSM for three values of the coupling constant.

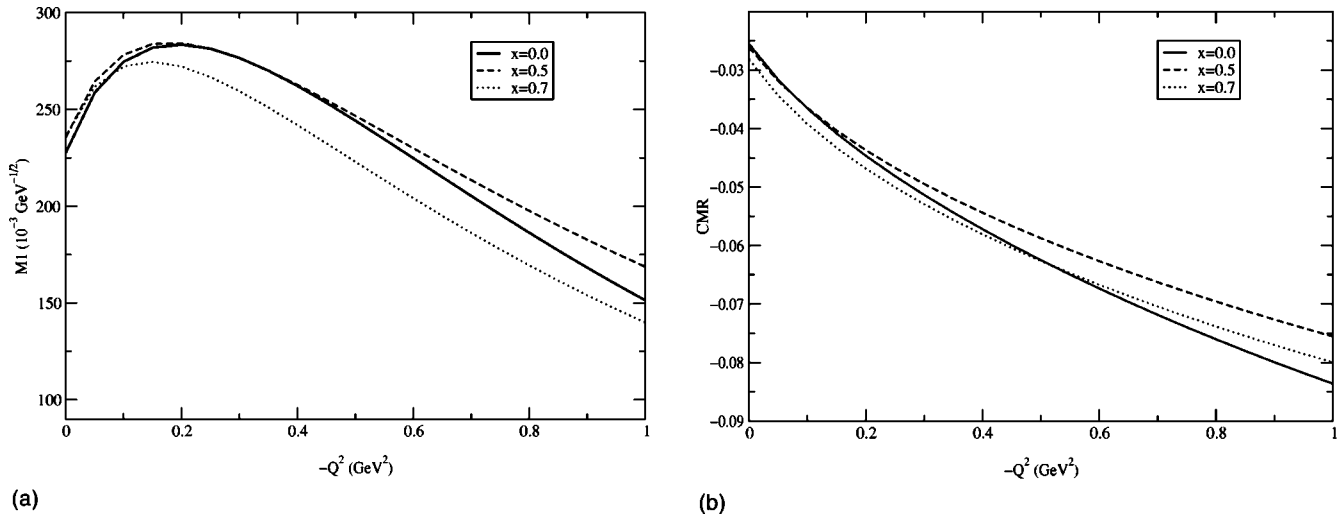

FIG. 7. $M1$ (left) and CMR (right) in the LSM, computed in different inertial frames using the standard parameter set in the LSM. The parameter x denotes the fraction of the photon momentum carried by the Δ.

$C2$ results from pion contribution alone, whereas $M1$ receives contributions from both pions and quarks. The stronger pion cloud enhances more $C2$ than $M1$ resulting in a larger (in absolute value) CMR for higher coupling constant. The same trends were also found in the CDM (but with even smaller variations with G).

Finally we address the problem of the reference frame. In principle, the theoretical amplitudes should not be dependent on the particular choice of the reference frame. However, due to the lack of translational invariance of the model baryon states (even when recoil corrections are taken into account), that is not the case. Nevertheless, no dramatic changes in the results, as a consequence of the different choice of reference frame, are supposed to occur. In Fig. 7 we present the $M1$ multipole amplitude and the CMR ratio for the LSM ($g=5.0$) and for three values of the parameter x which is the fraction of the photon momentum carried by the Δ: $x=0$, $x=0.5$, and $x=0.7$ (EMR follows the trend of CMR). The curve $x=0.5$ would correspond to the Breit frame if nucleon and Δ were degenerate. The major differences (indicating lack of covariance) come up at large values of $-Q^2$ as one would anticipate. Indeed, unlike the correct description of baryon motion through Lorentz boosts of zero momentum eigenstates as mentioned in Sec. II, our approximate treatment is *not* relativistic and, therefore, more reliable for small and intermediate linear momenta. The region spanned by the curves in Fig. 7 gives an idea of the ''theoretical uncertainty'' of the model predictions.

V. CONCLUSIONS

In this paper we addressed the question of the Δ electroproduction amplitudes in the framework of two chiral effective models of the nucleon with meson and quark degrees of freedom. Although the predictions for the ratios $E2/M1$ and $C2/M1$ are compatible with data in both models, the amplitudes are better reproduced in the LSM thus favoring a picture of the nucleon and the delta with a stronger pion cloud. Recoil corrections of the baryons were taken into account in this study but no dramatic change was actually found with respect to the calculation with just angular momentum projection from the hedgehog. This is different from the modifications occurring in nucleon form factors where larger effects were found when the center of mass motion spurious components are removed from the baryon wave functions. Strong fluctuations on $C2/M1$, as seen in the experimental data, are not observed in the present approach.

ACKNOWLEDGMENTS

We thank B. Golli, M. Rosina, S. Širca, A. Silva, and D. Urbano for useful discussions. Financial support from Fundação para a Ciência e Tecnologia, Portugal, Project No. PRAXIS/PCEX/P/FIS/6/96 is acknowledged. One of the authors (L.A.) also acknowledges the financial support to his Ph.D. program from PRODEP Project No. 185/007.

APPENDIX A: DEFINITION OF THE MAGNETIC AND ELECTRIC MULTIPOLE AMPLITUDES

The operator involved in the calculation of the transverse helicity amplitudes is

$$\hat{O}(\boldsymbol{r})=e^{-i\boldsymbol{q}\cdot\boldsymbol{r}}\boldsymbol{\epsilon}_1\cdot\boldsymbol{J}(\boldsymbol{r}). \tag{A1}$$

Choosing the z axis in the direction of $\boldsymbol{q}$, the expansion of the exponential reads

$$e^{-i\boldsymbol{q}\cdot\boldsymbol{r}}=\sqrt{4\pi}\sum_l\,(-i)^l\sqrt{2l+1}j_l(qr)Y_{l0}(\hat{\boldsymbol{r}}), \tag{A2}$$

where $j_l(x)$ are the spherical Bessel functions and $Y_{lm}(\hat{\boldsymbol{r}})$ are the spherical harmonics. Now, the product $Y_{l\mu}(\hat{\boldsymbol{r}})\boldsymbol{\epsilon}_\nu$ can be cast in terms of the vector spherical harmonics as

$$Y_{l\mu}(\hat{\boldsymbol{r}})\boldsymbol{\epsilon}_\nu=\sum_{jm}\,\langle l\mu;1\nu|jm\rangle\boldsymbol{Y}^m_{jl}(\hat{\boldsymbol{r}}), \tag{A3}$$

where $\langle l\mu;l'\mu'|jm\rangle$ are Clebsch-Gordan coefficients. Equation (A1) then reads

$$\hat{O}(\boldsymbol{r})=\sqrt{4\pi}\sum_{lj}\ (-i)^l\sqrt{2l+1}j_l(qr)\langle l0;11|j1\rangle \boldsymbol{Y}^1_{jl}(\hat{\boldsymbol{r}})\cdot\boldsymbol{J}(\boldsymbol{r}). \tag{A4}$$

Since only the terms with $j=l,\ j=l\pm1$ contribute, we may write

$$\begin{aligned}\hat{O}(\boldsymbol{r})&=\sqrt{2\pi}\sum_L\ \sqrt{2L+1}(-i)^L\Bigg\{-j_L(qr)\boldsymbol{Y}^1_{LL}(\hat{\boldsymbol{r}})\cdot\boldsymbol{J}(\boldsymbol{r})\\&\quad+i\Bigg[\sqrt{\frac{L+1}{2L+1}}j_{L-1}(qr)\boldsymbol{Y}^1_{LL-1}(\hat{\boldsymbol{r}})\cdot\boldsymbol{J}(\boldsymbol{r})\\&\quad-\sqrt{\frac{L}{2L+1}}j_{L+1}(qr)\boldsymbol{Y}_{LL+1}(\hat{\boldsymbol{r}})\cdot\boldsymbol{J}(\boldsymbol{r})\Bigg]\Bigg\}\\&=\sqrt{2\pi}\sum_L\ \sqrt{2L+1}(-i)^L\Bigg\{-j_L(qr)\boldsymbol{Y}^1_{LL}(\hat{\boldsymbol{r}})\\&\quad+\frac{1}{k}\boldsymbol{\nabla}[j_L(qr)\boldsymbol{Y}^1_{LL}(\hat{\boldsymbol{r}})]\Bigg\}\cdot\boldsymbol{J}(\boldsymbol{r})\end{aligned} \tag{A5}$$

(see Ref. [36] for more details). The two terms inside the curly braces in this expression are, respectively, the electromagnetic field $(L,1)$-magnetic and $(L,1)$-electric multipoles

$$\boldsymbol{A}^{(\mathcal{M})}_{LM}(\boldsymbol{r})=j_L(qr)\boldsymbol{Y}^M_{LL}(\hat{\boldsymbol{r}}), \tag{A6}$$

$$\boldsymbol{A}^{(\mathcal{E})}_{LM}(\boldsymbol{r})=-\frac{i}{k}\boldsymbol{\nabla}\times[j_L(qr)\boldsymbol{Y}^M_{LL}(\hat{\boldsymbol{r}})]. \tag{A7}$$

As is shown, for instance, in Ref. [36], the scalar products of the Lth order field multipoles with any vector (such as the current density operator) form the irreducible components of rank-L operators, with parity $(-1)^{L+1}$ and $(-1)^L$ for the magnetic and electric multipoles, respectively. In a transition between states with angular momentum $J_i=1/2$ and $J_f=3/2$ and positive parity, only $(L=1)$-magnetic and $(L=2)$-electric multipoles may contribute, so that the operator $\hat{O}$ may be replaced by

$$\hat{O}'(\boldsymbol{r})=i[\sqrt{6\pi}\boldsymbol{A}^{(\mathcal{M})}_{11}(\boldsymbol{r})-\sqrt{10\pi}\boldsymbol{A}^{(\mathcal{E})}_{21}(\boldsymbol{r})]\cdot\boldsymbol{J}(\boldsymbol{r}). \tag{A8}$$

The $M1$ and $E2$ amplitudes are, respectively, the matrix elements of the first and second terms on the right hand side of this equation. To make the correspondence with Eq. (34) we note that

$$\begin{aligned}i\sqrt{6\pi}\boldsymbol{A}^{(\mathcal{M})}_{11}(\boldsymbol{r})\cdot\boldsymbol{J}(\boldsymbol{r})&=\frac{3i}{\sqrt{2}}j_1(qr)\sum_{\mu\nu}\ \langle 1\mu;1\nu|11\rangle\hat{r}_\mu J_\nu(\boldsymbol{r})\\&=-\frac{3}{2}j_1(qr)[\hat{\boldsymbol{r}}\times\boldsymbol{J}(\boldsymbol{r})]_1,\end{aligned} \tag{A9}$$

where use was made of the definition of the vector spherical harmonics and of the expression of the spherical components of the vector product of two vectors. The scalar amplitude can be derived in a similar fashion.

APPENDIX B: TRANSITION OVERLAP

The transition overlap of two (not necessarily the same) hedgehog baryons, defined as

$$N(\boldsymbol{a},\Omega)=\langle\psi'_h|U(\boldsymbol{a})R(\Omega)|\psi_h\rangle, \tag{B1}$$

is a recurring function in calculations involving isospin and linear momentum projected states [11,24]. It is the following product of quark and meson overlaps:

$$N(\boldsymbol{a},\Omega)=N^3_q(\boldsymbol{a},\Omega)N_\pi(\boldsymbol{a},\Omega)N_\sigma(\boldsymbol{a},\Omega)N_\chi(\boldsymbol{a},\Omega).$$

An explicit form for this function can be derived following the calculation of the norm overlaps in Ref. [11]. The isoscalar meson overlaps do not depend on Ω or on the orientation of $\boldsymbol{a}$, and taking advantage of the properties of the coherent states (for the sigma field for instance), one obtains

$$\begin{aligned}N_\sigma(\boldsymbol{a},\Omega)&\equiv n_\sigma(a)\\&=\exp\Bigg\{g^\sigma_0(a)-\pi\int_0^\infty dkk^2\omega_\sigma(k)\\&\quad\times[\eta'^2(k)+\eta^2(k)]\Bigg\},\end{aligned} \tag{B2}$$

where we introduced the functions

$$g^\sigma_l(a)=2\pi\int_0^\infty dkk^2\omega_\sigma(k)j_l(ka)\eta'(k)\eta(k). \tag{B3}$$

A similar function should also be defined for the chromodielectric field. The quark overlap is also readily computed, because the spatial part of the quark wavefunctions is invariant under isospin rotations and the spin-isospin part is invariant under space translations. It is given by

$$N_q(\boldsymbol{a},\Omega)=n_q(a)\mathcal{N}_q(\Omega), \tag{B4}$$

$$n_q(a)=\frac{2}{\pi}\int_0^\infty dkk^2j_0(ka)[\tilde{u}'(k)\tilde{u}(k)+\tilde{v}'(k)\tilde{v}(k)], \tag{B5}$$

$$\mathcal{N}_q(\Omega)=\cos\frac{\beta}{2}\cos\frac{\alpha+\gamma}{2}. \tag{B6}$$

In these equations, $\tilde{u}$ and $\tilde{v}$ are Fourier transforms of the quark profiles, given by

$$\tilde{u}(k)=\int_0^\infty drr^2j_0(kr)u(r), \tag{B7}$$

$$\tilde{v}(k)=\int_0^\infty drr^2j_1(kr)v(r). \tag{B8}$$

For the pion field overlap, we get

$$N_\pi(\boldsymbol{a},\Omega)=\exp\left\{-\pi\int_0^\infty dk k^2\omega_\pi(k)[\xi'^2(k)+\xi^2(k)]\right\}\times\exp\left\{\frac{1}{3}[g_0^\pi(a)+g_2^\pi(a)]\mathrm{Tr}R(\Omega)\right\}\times\exp\{g_2^\pi(a)\hat{a}_i R_{ij}(\Omega)\hat{a}_j\},\tag{B9}$$

with g_l^π defined as for the σ [see Eq. (B3)]:

$$g_l^\pi(a)=2\pi\int_0^\infty dk\, k^2\omega_\pi(k)j_l(ka)\xi'(k)\xi(k).\tag{B10}$$

In the reference frame with the z axis along the axis of the rotation R, the quantity $\hat{a}_i R_{ij}(\Omega)\hat{a}_j$ does not depend on the azimuthal angle of vector $\boldsymbol{a}$ and that could be exploited in order to simplify some integrations [11]. However, the orientation of the z axis has already been fixed along the direction of the photon momentum. Therefore, in all integrations over $\boldsymbol{a}$ the transformation $\boldsymbol{a}\to\mathcal{T}^{-1}\boldsymbol{a}$ is made, where $\mathcal{T}$ is the rotation that aligns the z axis with the axis of the rotation $R(\Omega)$, and again advantage can be taken from the above-mentioned independence of the azimuthal angle. One gets

$$N_\pi(\mathcal{T}^{-1}\boldsymbol{a},\Omega)=n_\pi(a)\mathcal{N}_\pi(a,s,\Omega),\tag{B11}$$

where $s=\cos\theta_a$ is the cosine of the polar angle of $\boldsymbol{a}$, and

$$n_\pi(a)=\exp\left\{g_0^\pi(a)-\pi\int_0^\infty dk k^2\omega_\pi(k)[\xi'^2(k)+\xi^2(k)]\right\}\tag{B12}$$

$$\mathcal{N}_\pi(a,s,\Omega)=\exp\left\{2z(a,s)\left(\cos^2\frac{\beta}{2}\cos^2\frac{\alpha+\gamma}{2}-1\right)\right\}\tag{B13}$$

$$z(a,s)=\tfrac{2}{3}[g_0^\pi(a)+P_2(s)g_2^\pi(a)],\tag{B14}$$

$P_2(s)$ being the Legendre polynomial of second degree.

APPENDIX C: CALCULATION OF MATRIX ELEMENTS WITH PROJECTED STATES

Here we present some details regarding the calculation of matrix elements of operators between isospin and linear momentum projected states, using the $C2$ amplitude—see Eq. (36)—as an example. The other amplitudes can be obtained in a similar way (details in Ref. [37]).

The electromagnetic current density for the two effective theories considered in this paper, derived using Noether's theorem, reads

$$J^\mu(\boldsymbol{r})=\sum_{c=1}^3\overline{\psi}_{(c)}(\boldsymbol{r})\gamma^\mu\left(\frac{1}{6}+\frac{1}{2}\tau_0^{(c)}\right)\psi_{(c)}(\boldsymbol{r})+[\vec{\pi}(\boldsymbol{r})\times\partial^\mu\vec{\pi}(\boldsymbol{r})]_0,\tag{C1}$$

where c is a quark index and the cross product in the second term is in isospin space. The current density is the sum of an isoscalar operator

$$S^\mu(\boldsymbol{r})=\frac{1}{6}\sum_{c=1}^3\overline{\psi}_{(c)}(\boldsymbol{r})\gamma^\mu\psi_{(c)}(\boldsymbol{r}),\tag{C2}$$

which, because of isospin conservation, cannot contribute to N-Δ matrix elements, and the zeroth component of an isovector operator

$$V_{1,t}^\mu(\boldsymbol{r})=\frac{1}{2}\sum_{c=1}^3\overline{\psi}_{(c)}(\boldsymbol{r})\gamma^\mu\tau_t^{(c)}\psi_{(c)}(\boldsymbol{r})+[\vec{\pi}(\boldsymbol{r})\times\partial^\mu\vec{\pi}(\boldsymbol{r})]_t.\tag{C3}$$

The components of isovector operators commute in a well defined manner with the isospin-space rotations involved in the isospin projectors (see Ref. [38], for instance) and one can show that, regarding the expression of the $C2$ amplitude,

$$\mathcal{P}^{3/2^\dagger}_{1/2,-1/2}V^0_{10}(\boldsymbol{r})\mathcal{P}^{1/2}_{1/2,-1/2}=\sum_t c_t V^0_{1t}(\boldsymbol{r})\mathcal{P}^{1/2}_{-(t+1/2),-1/2},\tag{C4}$$

with

$$c_t=\sqrt{\frac{2}{3}}\left\langle\frac{1}{2},t+\frac{1}{2};1,-t\middle|\frac{3}{2}\frac{1}{2}\right\rangle.\tag{C5}$$

We can then write the $C2$ amplitude as

$$M^{C2}(q)=-\frac{\sqrt{10\pi}}{(2\pi)^2}N_{N\Delta}\sum_t c_t\int d^3\boldsymbol{a}\int d\Omega\times\mathcal{D}^{1/2*}_{-(1/2+t),-1/2}(\Omega)F_t(\boldsymbol{a},\Omega),\tag{C6}$$

with

$$F_t(\boldsymbol{a},\Omega)=\int d^3\boldsymbol{r}j_2(qr)Y_{20}(\hat{\boldsymbol{r}})\times\langle\psi_h(\Delta)|U^\dagger[(x-1)\boldsymbol{a}]V^0_{1t}(\boldsymbol{r})R(\Omega)U(x\boldsymbol{a})|\psi_h(N)\rangle.\tag{C7}$$

In this expression, $|\psi_h(N)\rangle$ and $|\psi_h(\Delta)\rangle$ represent the nucleon and the delta hedgehogs.

The quark component of the isovector part of the charge density in Eq. (C3) cannot contribute here since the $C2$ is a matrix element of an $L=2$ operator between s-wave quark states. We are then left only with the pion contribution to the charge density, and we expand the pion field $\vec{\pi}(\boldsymbol{r})$ and its canonical conjugate $\vec{P}_\pi(\boldsymbol{r})$ in plane waves

$$\pi_i(\boldsymbol{r})=\frac{1}{(2\pi)^{3/2}}\int d^3\boldsymbol{k}\frac{1}{\sqrt{2\omega_\pi(k)}}[a_i(\boldsymbol{k})e^{i\boldsymbol{k}\cdot\boldsymbol{r}}+a_i^\dagger(\boldsymbol{k})e^{-i\boldsymbol{k}\cdot\boldsymbol{r}}],\tag{C8}$$

$$P_{\pi i}(\boldsymbol{r}) = \frac{i}{(2\pi)^{3/2}} \int d^3\boldsymbol{k} \sqrt{\frac{\omega_\pi(k)}{2}} [a_i(\boldsymbol{k}) e^{i\boldsymbol{k}\cdot\boldsymbol{r}} - a_i^\dagger(\boldsymbol{k}) e^{-i\boldsymbol{k}\cdot\boldsymbol{r}}]. \tag{C9}$$

The translations and/or isorotations of coherent states still yield coherent states (the transformed states are still eigenstates of the annihilation operators) with shifted and/or isorotated amplitudes. Indeed, for the pion field one has

$$a_i(\boldsymbol{k}) U(x\boldsymbol{a}) R(\Omega) |\psi_h(N)\rangle = \sqrt{\frac{\omega_\pi(k)}{2}} e^{-ix\boldsymbol{k}\cdot\boldsymbol{a}} R_{ij}(\Omega) \xi_j^{(N)}(\boldsymbol{k}) U(x\boldsymbol{a}) R(\Omega) |\psi_h(N)\rangle, \tag{C10}$$

$$\langle \psi_h(\Delta) | U^\dagger[(x-1)\boldsymbol{a}] a_i(\boldsymbol{k}) = \sqrt{\frac{\omega_\pi(k)}{2}} e^{i(x-1)\boldsymbol{k}\cdot\boldsymbol{a}} \xi_i^{(\Delta)}(\boldsymbol{k}) \langle \psi_h(\Delta) | U^\dagger[(x-1)\boldsymbol{a}]. \tag{C11}$$

Taking now advantage of the hedgehog shape of the pion coherent state amplitude, Eq. (18), we can write the Cartesian components of the functions $F_t(\boldsymbol{a},\Omega)$ in Eq. (C7) as

$$F_i(\boldsymbol{a},\Omega) = -\frac{i}{2\pi} N(\boldsymbol{a},\Omega) \int d^3\boldsymbol{r} j_2(qr) Y_{20}(\hat{\boldsymbol{r}}) \epsilon_{ijk} R_{kl}(\Omega) \times (r_-)_l (r_+)_j \alpha(a,r,\hat{\boldsymbol{a}}\cdot\hat{\boldsymbol{r}}), \tag{C12}$$

where

$$\boldsymbol{r}_+ = \boldsymbol{r} + (1-x)\boldsymbol{a}, \tag{C13}$$

$$\boldsymbol{r}_- = \boldsymbol{r} - x\boldsymbol{a}, \tag{C14}$$

$$\alpha(a,r,\hat{\boldsymbol{a}}\cdot\hat{\boldsymbol{r}}) = \frac{A_N(r_-) B_\Delta(r_+) + A_\Delta(r_+) B_N(r_-)}{r_- r_+}, \tag{C15}$$

$$A_B(r) = \int dk k^2 j_1(kr) \xi_B(k), \tag{C16}$$

$$B_B(r) = \int dk k^2 \omega_\pi(k) j_1(kr) \xi_B(k), \tag{C17}$$

and

$$N(\boldsymbol{a},\Omega) = \langle \psi_h(\Delta) | U(\boldsymbol{a}) R(\Omega) | \psi_h(N) \rangle \tag{C18}$$

is the transition overlap of the N and the Δ intrinsic hedgehogs, derived in Appendix B.

Expanding the products $(r_-)_l (r_+)_j$, the function (C12) unfolds in three terms:

$$F_i(\boldsymbol{a},\Omega) = F_i^{(0)}(\boldsymbol{a},\Omega) + F_i^{(1)}(\boldsymbol{a},\Omega) + F_i^{(2)}(\boldsymbol{a},\Omega), \tag{C19}$$

with

$$F_i^{(0)}(\boldsymbol{a},\Omega) = \frac{i}{2\pi} N(\boldsymbol{a},\Omega) a^2 x(1-x) \epsilon_{ijk} R_{kl}(\Omega) \hat{a}_j \hat{a}_l \times \int d^3\boldsymbol{r} j_2(qr) Y_{20}(\hat{\boldsymbol{r}}) \alpha(a,r,\hat{\boldsymbol{a}}\cdot\hat{\boldsymbol{r}}), \tag{C20}$$

$$F_i^{(1)}(\boldsymbol{a},\Omega) = -\frac{i}{2\pi} N(\boldsymbol{a},\Omega) a \epsilon_{ijk} R_{kl}(\Omega) \int d^3\boldsymbol{r} r j_2(qr) Y_{20}(\hat{\boldsymbol{r}}) \times [(1-x)\hat{a}_j \hat{r}_l - x\hat{a}_l \hat{r}_j] \alpha(a,r,\hat{\boldsymbol{a}}\cdot\hat{\boldsymbol{r}}), \tag{C21}$$

$$F_i^{(2)}(\boldsymbol{a},\Omega) = -\frac{i}{2\pi} N(\boldsymbol{a},\Omega) \epsilon_{ijk} R_{kl}(\Omega) \int d^3\boldsymbol{r} r^2 j_2(qr) \times Y_{20}(\hat{\boldsymbol{r}}) \hat{r}_l \hat{r}_j \alpha(a,r,\hat{\boldsymbol{a}}\cdot\hat{\boldsymbol{r}}). \tag{C22}$$

Let us focus on $F_i^{(0)}$. In doing the integration over $\boldsymbol{r}$ we are not allowed to pick any particularly convenient orientation for the vector $\boldsymbol{a}$, whose components are also integration variables. Still, it is possible to perform the integration over the azimuthal angle of $\boldsymbol{r}$ analytically, yielding

$$F_i^{(0)}(\boldsymbol{a},\Omega) = \frac{i}{4} \sqrt{\frac{5}{\pi}} x(1-x) a^2 S_{02}(a) \epsilon_{ijk} \times R_{kl}(\Omega) N(\boldsymbol{a},\Omega) (3\hat{a}_3^2 - 1) \hat{a}_j \hat{a}_l, \tag{C23}$$

where the following functions were introduced:

$$S_{nl}(a) = \int_0^\infty dr r^{2+n} j_2(qr) \int_{-1}^1 du P_l(u) \alpha(a,r,u), \tag{C24}$$

$P_l(u)$ are the Legendre polynomials and $u = \cos\theta_r$ is the cosine of the polar angle of $\boldsymbol{r}$. Further analytical refinations of these F functions are not possible because the function $\alpha(a,r,u)$ depends on the radial profiles of the meson fields, which are known only numerically.

In order to compute the contribution of the function $F^{(0)}$ to M^{C2}, we replace its spherical components in Eq. (C6). Making the transformation $\boldsymbol{a} \to \mathcal{T}^{-1}\boldsymbol{a}$ (see Appendix B) the dependence of the integrand on the azimuthal orientation of the vector $\boldsymbol{a}$ is restricted to the terms $\hat{a}_j \hat{a}_l$ and $\hat{a}_3^2 \hat{a}_j \hat{a}_l$, allowing us to perform the integration over ϕ_a analytically. The contribution of $F^{(0)}$ to the Coulomb amplitude can then be written as

$$M^{C2^{(0)}}(q) = -\frac{\sqrt{10\pi}}{(2\pi)^2} N_{N\Delta} \sum_t c_t \int_0^\infty da a^2 \int_{-1}^1 ds \times \int d\Omega \mathcal{D}^{1/2*}_{-(1/2+t)-1/2}(\Omega) I_t^{(0)}(a,s,\Omega), \tag{C25}$$

where $s = \cos\theta_a$ is the cosine of the polar angle of $\boldsymbol{a}$ and

$$I_t^{(0)} = \int_0^{2\pi} d\phi_a F_t^{(0)}(\mathcal{T}^{-1}\boldsymbol{a},\Omega). \tag{C26}$$

The integration over the azimuthal angle of $\boldsymbol{a}$ can now be performed analytically, as the dependence on this variable only appears in the vector component products such as $\hat{a}_j\hat{a}_l$, etc. The cartesian components of the isovector function $I^{(0)}$ are then

$$\begin{aligned} I_i^{(0)}(a,s,\Omega) = i\sqrt{\frac{5\pi}{4}}x(1-x)a^2 S_{02}(a)n(a)N(a,s,\Omega) \\ \times\Bigg\{ 3P_4(s)T_i(\Omega) - \frac{1}{3}[P_0(s)-P_2(s)] \\ \times X_i(\Omega) - P_2(s)W_i(\Omega) \\ + \frac{1}{35}[7P_0(s)-10P_2(s)+3P_4(s)] \\ \times[2Y_i(\Omega)+X_i(\Omega)] + \frac{3}{7}[P_2(s)-P_4(s)] \\ \times[2Z_i(\Omega)+2V_i(\Omega)+W_i(\Omega)+U_i(\Omega)]\Bigg\}, \end{aligned} \tag{C27}$$

where

$$N(a,s,\Omega) = N(\mathcal{T}^{-1}\boldsymbol{a},\Omega) \tag{C28}$$

(see Appendix B) and the following isovectors, functions of the Euler angles alone, have been introduced:

$$T_i(\Omega) = \epsilon_{ijk}R_{kl}(\Omega)T_{3j}(\Omega)T_{3l}(\Omega)T_{33}^2(\Omega),$$

$$U_i(\Omega) = \epsilon_{ijk}R_{kj}(\Omega)T_{33}^2(\Omega),$$

$$V_i(\Omega) = \epsilon_{ijk}R_{k3}(\Omega)T_{3j}(\Omega)T_{33}(\Omega),$$

$$W_i(\Omega) = \epsilon_{ijk}R_{kl}(\Omega)T_{3j}(\Omega)T_{3l}(\Omega),$$

$$X_i(\Omega) = \epsilon_{ijk}R_{kj}(\Omega),$$

$$Y_i(\Omega) = \epsilon_{i3k}R_{k3}(\Omega),$$

$$Z_i(\Omega) = \epsilon_{i3k}R_{kl}(\Omega)T_{3l}(\Omega)T_{33}(\Omega).$$

In these definitions, T_{ij} are the matrix elements of the transformation $\mathcal{T}$. We now note that $R_{kl}T_{3l} = T_{ks}^{-1}T_{sk'}R_{k'l}T_{l3}^{-1} = T_{3k}$, because $T_{sk'}R_{k'l}T_{l3}^{-1} = R_{s3}^{(z)} = \delta_{s3}$ is the rotation matrix transformed to the frame in which the z axis is along the axis of rotation. Then, we immediately obtain $T_i = 0$, $W_i = 0$ and $Z_i = \epsilon_{i3k}T_{3k}T_{33}$. Finally, we reconstruct the spherical components of $I^{(0)}$, replace the result in Eq. (C25) and, after the contraction with the Wigner matrices $\mathcal{D}$, the integration over the Euler angles can proceed analytically, along the lines followed in Ref. [11]. The final result is

$$\begin{aligned} M^{C2^{(0)}}(q) = \frac{\pi}{6\sqrt{2}}x(1-x)N_{N\Delta}\int_0^\infty da a^4 n(a)S_{02}(a) \\ \times[T_{10}(a) - T_{12}(a) - T_{30}(a) + T_{32}(a)], \end{aligned} \tag{C29}$$

with T_{kl} defined by

$$T_{kl}(a) = \int_{-1}^{1} ds \frac{e^{-z}}{z} I_k(z)P_l(s), \tag{C30}$$

where I_k are the modified Bessel functions of the first kind, depending on the parameter z introduced in Eq. (B14). Using a similar procedure we computed the two remaining contributions to the scalar amplitude. The whole method can be applied to obtain formulas for the magnetic dipole amplitude [37].

[1] S.A. Gogilidze *et al.*, Yad Fiz. **45**, 1085 (1987) [Sov. J. Nucl. Phys. **45**, 674 (1987)].
[2] M. Warns *et al.*, Z. Phys. C **45**, 627 (1990).
[3] S. Capstick and G. Karl, Phys. Rev. D **41**, 2767 (1990); S. Capstick and B.D. Keister, *ibid.* **51**, 3598 (1995).
[4] M. Bourdeau and N.C. Mukhopadhyay, Phys. Rev. Lett. **58**, 976 (1987).
[5] K. Bermuth *et al.*, Phys. Rev. D **37**, 89 (1988).
[6] M. Fiolhais, B. Golli, and S. Širca, Phys. Lett. B **373**, 229 (1996).
[7] D. Lu, A. Thomas, and A. Williams, Phys. Rev. C **55**, 3108 (1997).
[8] M. Birse, M. Banerjee, Phys. Lett. **136B**, 284 (1984); Phys. Rev. D **31**, 118 (1985); S. Kahana, G. Ripka, and V. Soni, Nucl. Phys. **A415**, 351 (1984).
[9] H. Pirner, Prog. Part. Nucl. Phys. **29**, 33 (1992); M. Birse, *ibid.* **25**, 1 (1990).
[10] M. Fiolhais *et al.*, Nucl. Phys. **A481**, 727 (1988).
[11] T. Neuber *et al.*, Nucl. Phys. **A560**, 909 (1993).
[12] B. Golli and M. Rosina, Phys. Lett. **165B**, 347 (1985); M. C. Birse, Phys. Rev. D **33**, 1934 (1986).
[13] E. G. Lübeck *et al.*, Phys. Rev. D **33**, 234 (1986).
[14] A. Drago, M. Fiolhais, and U. Tambini, Nucl. Phys. **A609**, 488 (1996).
[15] A. Buchmann, E. Hernandez, and A. Faessler, Phys. Rev. C **55**, 448 (1997); A. Buchmann, Z. Naturforsch., A: Phys. Sci. **52**, 877 (1997); A. Buchmann *et al.* Phys. Rev. C **58**, 2478 (1998).
[16] A. Wirzba and W. Weise, Phys. Lett. B **188**, 6 (1987).
[17] H. Walliser and G. Holzwarth, Z. Phys. A **357**, 317 (1997).
[18] T. Watabe, Chr. V. Christov, and K. Goeke, Phys. Lett. B **349**, 197 (1995).
[19] A. Silva *et al.*, Nucl. Phys. **A675**, 637 (2000).
[20] A. Drago, M. Fiolhais, and U. Tambini, Nucl. Phys. **A588**, 801 (1995).
[21] L. Amoreira *et al.*, Int. J. Mod. Phys. A **14**, 731 (1999).
[22] L. Amoreira *et al.*, J. Phys. G **21**, 1657 (1995); M. Čibej *et al.*, *ibid.* **18**, 49 (1992).

[23] E. Ruiz Arriola *et al.*, Z. Phys. A **333**, 203 (1989).
[24] T. Neuber and K. Goeke, Phys. Lett. B **281**, 202 (1992).
[25] P. Alberto *et al.*, Z. Phys. A **336**, 449 (1990).
[26] T.W. Donnelly and A.S. Raskin, Ann. Phys. (N.Y.) **169**, 247 (1986); **191**, 78 (1989).
[27] R. Siddle *et al.*, Nucl. Phys. **B34**, 93 (1971); J. Adler *et al.*, *ibid.* **B46**, 573 (1972); K. Bätzner *et al.*, *ibid.* **B76**, 1 (1974).
[28] C. Mistretta *et al.*, Phys. Rev. **184**, 1487 (1968); S. Galster *et al.*, Phys. Rev. D **5**, 519 (1972).
[29] R. Arnt *et al.*, Phys. Rev. C **56**, 577 (1997); R. Beck *et al.*, Phys. Rev. Lett. **78**, 606 (1997); G. Blanpield *et al.*, *ibid.* **79**, 4337 (1997).
[30] R.W. Gothe, Proceedings of the International School of Nuclear Physics, 21st Course: ''Electromagnetic Probes and the Structure of Hadrons and Nuclei,'' Erice 1999 [Prog. Part. Nucl. Phys. (to be published)]; F. Kalleicher *et al.*, Z. Phys. A **359**, 201 (1997).
[31] H. Schmieden, Nucl. Phys. **A663–664**, 21 (2000).
[32] R.L. Crawford, Nucl. Phys. **B28**, 573 (1971).
[33] C. Mertz *et al.*, nucl-ex/9902012; G.A. Warren *et al.*, Phys. Rev. C **58**, 3722 (1998).
[34] W. Ash *et al.*, Phys. Lett. **24B**, 154 (1967); W. Bartel *et al.*, *ibid.* **28B**, 148 (1968); S. Stein *et al.*, Phys. Rev. D **12**, 1884 (1975).
[35] Particle Data Group, C. Caso *et al.*, Eur. Phys. J. C **3**, 1 (1998).
[36] J.M. Eisenberg and W. Greiner, *Nuclear Theory, Vol. 2: Excitation Mechanisms of the Nucleus* (North-Holland, Amsterdam, 1970).
[37] L. Amoreira, Ph.D. thesis, University of Beira Interior, 2000.
[38] A.R. Edmonds, *Angular Momentum in Quantum Mechanics* (Princeton University, Princeton, 1960).